Power-angle modulation controller to support transient stability of power systems dominated by power electronic interfacedwind generation

Perilla, Arcadio; Torres, José Luis Rueda; Papadakis, Stelios; Rakhshani, Elyas; van der Meijden, Mart; Gonzalez-Longatt, Francisco

DOI
10.3390/en13123178

Publication date
2020

Document Version
Final published version

Published in
Energies

Citation (APA)
Perilla, A., Torres, J. L. R., Papadakis, S., Rakhshani, E., van der Meijden, M., & Gonzalez-Longatt, F. (2020). Power-angle modulation controller to support transient stability of power systems dominated by power electronic interfacedwind generation. *Energies*, *13*(12), 1-21. Article en13123178. https://doi.org/10.3390/en13123178

energies

MDPI

Article

Power-Angle Modulation Controller to Support Transient Stability of Power Systems Dominated by Power Electronic Interfaced Wind Generation

Arcadio Perilla [1,*], José Luis Rueda Torres [1], Stelios Papadakis [1], Elyas Rakhshani [1], Mart van der Meijden [2] and Francisco Gonzalez-Longatt [3]

1 Electrical Sustainable Energy Department, Delft University of Technology, 2628 CD Delft, The Netherlands; J.L.RuedaTorres@tudelft.nl (J.L.R.T.); spapadakis92@gmail.com (S.P.); elyas.rakhshani@gmail.com (E.R.)
2 TenneT TSO B.V, 6812AR Arnhem, The Netherlands; Mart.vander.Meijden@tennet.eu
3 Department of Electrical Engineering, University of South-Eastern Norway, 3679 Notodden, Norway; F.Gonzalez-Longatt@usn.no
* Correspondence: a.perilla@tudelft.nl

Received: 3 May 2020; Accepted: 10 June 2020; Published: 19 June 2020

Abstract: During the last few years, electric power systems have undergone a widespread shift from conventional fossil-based generation toward renewable energy-based generation. Variable speed wind generators utilizing full-scale power electronics converters are becoming the preferred technology among other types of renewable-based generation, due to the high flexibility to implement different control functions that can support the stabilization of electrical power systems. This paper presents a fundamental study on the enhancement of transient stability in electrical power systems with increasing high share (i.e., above 50%) of power electronic interfaced generation. The wind generator type IV is taken as a representative form of power electronic interfaced generation, and the goal is to investigate how to mitigate the magnitude of the first swing while enhancing the damping of rotor angle oscillations triggered by major electrical disturbances. To perform such mitigation, this paper proposes a power-angle modulation (PAM) controller to adjust the post-fault active power response of the wind generator type IV, after a large disturbance occurs in the system. Based on a small size system, the PAM concept is introduced. The study is performed upon time-domain simulations and analytical formulations of the power transfer equations. Additionally, the IEEE 9 BUS system and the test model of Great Britain's system are used to further investigate the performance of the PAM controller in a multi-machine context, as well as to perform a comparative assessment of the effect of different fault locations, and the necessary wind generators that should be equipped with PAM controllers.

Keywords: transient stability; wind generator type IV; MIGRATE H2020 Project; renewable energy

1. Introduction

The integration of dispersed renewable power generation into the electrical power systems is becoming an undeniable reality that is being analyzed by the scientific community in many ways (cf. [1,2]), and one of the most critical issues is to keep acceptable performance of the rotor angle when a major disturbance occurs. This issue, known as transient stability, concerns the ability of the power system to ensure that synchronism is kept in all synchronous generators in operation when a large electrical disturbance, like a three-phase short circuit, occurs at any time [3]. Under such circumstances, the mechanical and electrical torques mismatch, and this may cause acceleration/deceleration in some synchronous generators. Therefore, transient instability can eventually cause undesirable events like generator outages, load shedding, and significant power disruptions.

The dynamics of the rotor angle of a synchronous generator are attached to the dynamics of the electromagnetic power at the generator's terminal bus, through the internal flux linkage [3]. This causes a prompt response of the rotor angle position due to the fluctuation of the output (electrical) power. Such a response occurs in the form of absorbing/releasing kinetic energy. The kinetic energy deployment affects the post-disturbance power flows and, therefore, is key to preventing transient instability. By contrast, type IV wind generators (WG) (which are being used to replace fossil fuel power plants with synchronous generators) are not electromagnetically coupled with the power system transients. This is due to the fact that the energy conversion process in a WG unit is performed through a power electronic converter that generally maximizes the power provided to the electrical networks through the maximum power pointing track (MPPT) control [4,5].

Currently, there are several studies that highlight negative and positive implications for the transient stability performance of electrical power systems by considering a massive integration of power electronics-interfaced generation units. For instance, according to some articles, the displacement of synchronous generators by wind generators (or any type of power electronic converter interfaced generation) can to deteriorate the transient stability performance [6]. Moreover, by regulating wind generator's power output, it can be possible to mitigate the torque imbalance (affecting the post-disturbance transient stability) of synchronous generators [7,8]. Control methods for transient stability of electrical power system, having fully decoupled wind generators, can be defined from different perspectives: (i) by adding hardware components (e.g., crowbar, fault current limiter); (ii) by modifying the outer control schemes of the grid side power electronic converters of the WGs.

Some research efforts have focused on the addition of an energy storage system (ESS) on the direct-current (DC) link of the fully decoupled WG to smooth the power output oscillations and enhance the low voltage ride through (LVRT) capability for the WG [9]. In [10] a static synchronous compensator (STATCOM) based method has been proposed to enhance LVRT capability of four parallel-operated fully decoupled WGs fed to a power system by a proportional–integral–derivative (PID) damping controller designed based on the modal control theory. Other methods based on hardware could incur substantial capital investments, without ensuring effectiveness and robustness. Therefore, this paper focuses on modifying the outer control scheme of the WGs. Other methods of existing literature attempted to modify the form of performing current limitations on the grid side converter, whereas other methods have proposed to modify the form of active and reactive power injection (e.g., based on signals measured at the connection point of the WGs). Alternatively, the reduction of active current has been implemented by adding supplementary signal (depended on DC link current) to compensate the torque imbalance [11]. In [12], the authors proposed to coordinate control of the injections of active and reactive powers by WGs as a mitigation solution for transient instability. A stability index was also proposed in [12] to estimate the proximity to instability, which is used to trigger the coordinated control scheme. In [13], a method based on vector current control is proposed, in which a decoupled and gain-scheduling controller is implemented in the outer loop of the grid side converter. The goal of such a vector current control is to preclude interactions that can involve the active power control and the voltage control. This situation can occur when a fully decoupled WG operates close to its nominal power, and is part of a weak transmission system.

In [14], a sensitivity analysis of active and reactive power injection by type 4 renewable power generation is shown. It is also shown that currently, some Europeans grid codes for WGs establish that when a fault event occurs in the power system, the injection of additional reactive current, (defined as a function of the voltage deviation experienced by the WG) should be executed based on a propotional control action. Furthermore, in [14], it is suggested that the amount of active current injection supplied (during the post fault period) should transiently provide ten times (or less) the nominal active power of the WG if, a linear ramp-rate (or active power gradient) controller, is utilized.

A supplementary control scheme for a grid side converter of a WG unit is proposed in [15] to simultaneously adjust the active and reactive power injection to prevent first-swing transient instability issues. Based on modal analysis, this study also suggests that the use of remote signals related to the

rotor angle of synchronous generators could be an attractive option for the development of future methods for transient stability enhancement. Nevertheless, there is a lack of insight into which and how these signals might be used, and what are the implications for the dynamic (rotor angle) response of synchronous generators due to the use of a remote signal. Moreover, the effectiveness of such approach in power systems with a high share of power electronic-interfaced wind generations remains as an open research line. It is worth pointing out that the active and reactive power adjustment methods presented in existing literature usually consider case studies with test systems having a share of renewable power generation up to 50%.

This paper bridges the research gap on how to mitigate the amplitude of the first swing while enhancing the damping of rotor angle oscillations triggered by major electrical disturbances. To this aim, a power-angle modulation (PAM) controller is proposed to adjust the post-fault active power response of the WG system type IV. Based on different test systems with different dynamic properties, a fundamental study based on time-domain simulations and analytical formulations of the power transfer equations is provided to thoroughly investigate the effectiveness of the level of support provided by the PAM controller, when it is used to safeguard the transient stability of a power system when increasing the share of renewable power generation above 50%.

The structure of the paper is as follows: based on a small-size test system and the analytical formulation of the power transfer equation, Section 2 provides a discussion on the need and expected effect of a PAM controller. Section 3 presents the implementation of the PAM controller on a generic model of a type IV WG. Several fault locations are considered to assess the effectiveness (i.e., reduction of rotor angle first swing and contribution to rotor angle oscillation damping) of the PAM controller in a small-size benchmark system (Section 3) and in a multi-machine power system represented by a synthetic model of Great Britain (Section 4). Finally, concluding remarks are given in Section 5.

2. The Principle of the Power-Angle Modulation (PAM) Method

The enhancement of the transient stability in power systems through power electronics devices located at transmission levels has been commonly tackled by utilizing Flexible AC Transmission Systems (FACTS) devices. In short, the enhancement of the transient stability is achieved by inducing a change in the power transferred (i.e., power-angle curve characteristics) by the synchronous generator (SG) connected to the power system. For instance, the Unified Power Flow Controller (UPFC) represents one of the applications (for FACTS devices) in which the PAM method has been explored [16]. The use of this method has revealed that a certain level of transient stability support is provided, but it is limited since the FACTS devices can only modify the quadrature's projection of the (induced) boosted voltage over the power system network [16]. However, this limitation (in the transient stability support) can potentially be overcome by the use of voltage source converters (VSC) units, which are those responsible for the energy conversion process in modern WG units type IV. Thus, the PAM method can still be applicable for providing an effective transient stability support if a PAM controller is designed taking into account the industrial practices requested nowadays (in Grid-Side VSC of type IV WG units), when a large disturbance occurs in the power system. Therefore, the development of the PAM controller's design requires the description of the following three aspects: first, the description of the expected dynamic performance of a type IV WG unit, during fault conditions. Second, the formulation of the steady-state power-angle curve's characteristics of the SG unit to be supported under several wind power and network strength conditions and third, the real-time use of the wide-area monitoring data available in the power system. The description of these aspects is presented in Sections 2.1, 2.2 and 3.

2.1. Steady-State Analysis of Wind Power Levels and Network Strength Conditions over the Power-Angle Curve's Characteristics

For the sake of illustration of the PAM concept, the analysis of the power-angle relationship of a power system dominated by power electronic-interfaced wind generation considers a reduced size power system model as shown in Figure 1. The external interconnected power system is described by an

infinite bus system, represented as a Thevenin equivalent circuit (e.g., voltage source G_{Ref}, and reactance x_2). The model also includes a conventional generation unit represented by a round rotor synchronous generator unit G1, and a wind power plant WG1. Both power plants have comparably rated powers and form a so-called Hybrid Generation Area 1 (HGA1). Thereafter, the HGA is understood as a synchronous area in which the power supply can be fully or mostly covered by either conventional generation (G1) or power electronic interfaced wind generation (WG1).

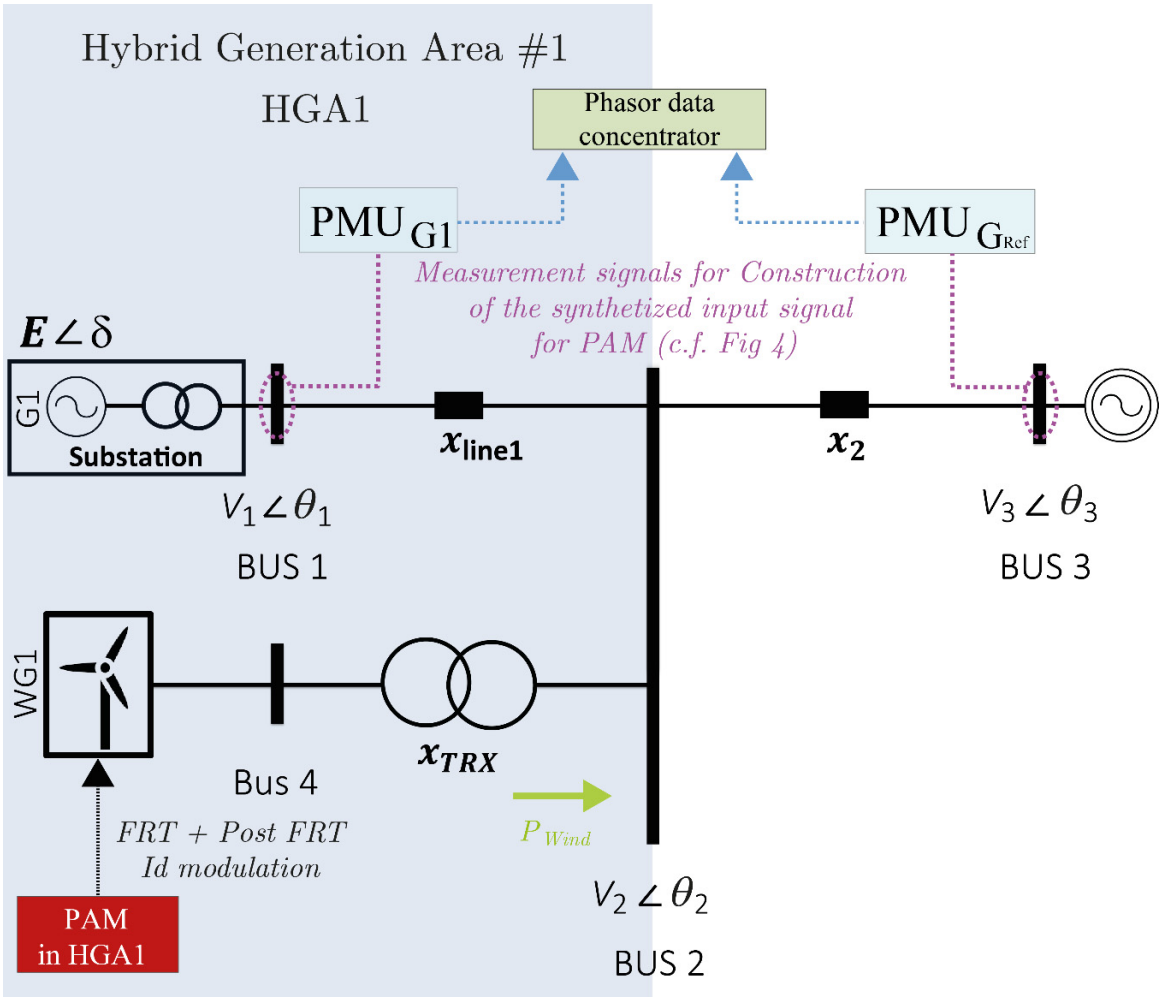

Figure 1. The reduced size power system model presenting the hybrid generation area (HGA) configuration, the equivalent network representation and the phasor measurement units (PMUs) used for enabling the operation of the power-angle modulation (PAM) controller added into the WG1 unit.

For a given active power dispatch of G1, it is assumed that the excitation control system maintains a constant magnitude for the internal electromotive force of G1. Moreover, following a common operational practice [17] to prevent a voltage haunting issue at the point of common coupling (PCC) BUS 2, for any active power dispatch of WG1, the WG1 unit is set to operate at unity power factor.

The power flow equations for the power system presented in Figure 1 are presented in the following equations:

$$x_1 = x_{Substation} + x_{line1} \tag{1}$$

$$P_{e_{SG}} = \frac{EV_2}{x_1}\sin(\delta - \theta_2) \tag{2}$$

$$P_{NET} = \frac{V_2 V_3}{x_2}\sin(\theta_2 - \theta_3) \tag{3}$$

$$P_{Wind} = P_{NET} - P_{e_{SG}} \tag{4}$$

where (1) represents the total impedance between the SG and the PCC (c.f., Figure 1). (2) indicates that the active power provided by G1 (i.e., $P_{e_{SG}}$) depends on the reactance x_1 and the angular difference $\delta - \theta_2$. However, if Equations (3) and (4) are analyzed together, it turns out that the phase angle θ_2, is a function of P_{Wind} and x_2. Therefore, the modulation of P_{Wind} can potentially induce an alteration of the electrical power magnitude $P_{e_{SG}}$, thereby attempting to support (i.e., mitigate rotor angle oscillations) G1 when it experiences power imbalances due to a large disturbance.

As shown in Figure 2, the degree of influence of P_{Wind} (from the point of view of the steady-state of power-angle relationships) over $P_{e_{SG}}$ is determined by the x_1 and x_2 ratios. Without wind power generation ($P_{Wind} = 0$ pu), Figure 2a shows that the power transferred by G1 is *shaped* by the reactances ratio x_2/x_1. However, with non-zero wind power generation (e.g., $P_{Wind} = 0.5$ pu), Figure 2b shows that wind power causes an additional effect over the power-angle curve. This effect can be perceived as a displacement of the power-angle curves (i.e., in amplitude and phase), lowering significantly the active power transferred by G1. It is also observed in Figure 2b that the magnitude reduction of the power-angle curve is more pronounced than the magnitude reduction observed in Figure 2a when the x_2/x_1 ratio is closer to one.

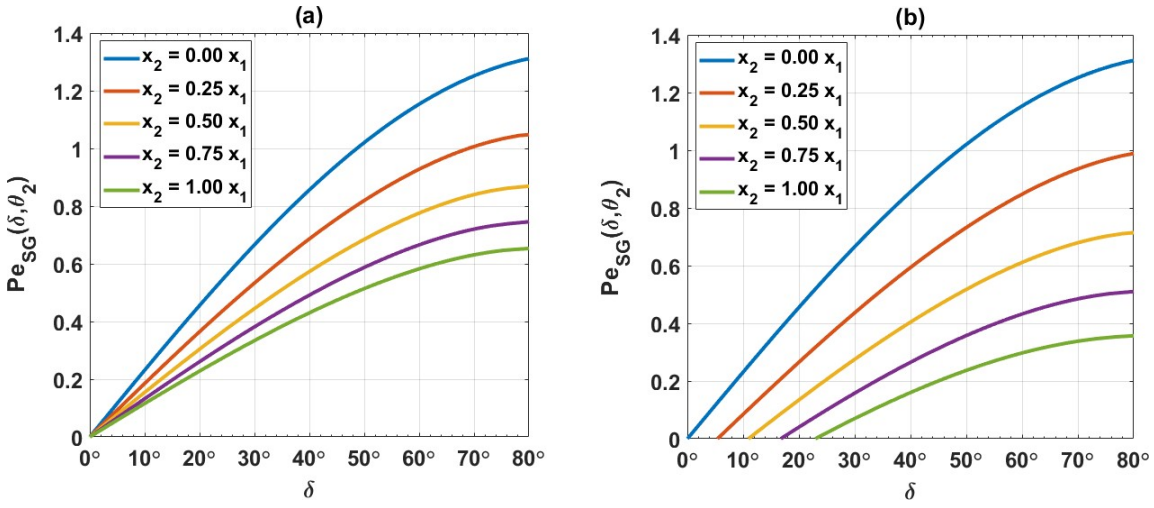

Figure 2. The power-angle curves of the synchronous generator SG1 are exhibited under different x_1 and x_2 ratios: (**a**) the active power provided by the WG1 unit is null, (**b**) the active power provided by the wind generator WG1 unit has been increased to 50% of the SG1 rated power.

Following the analysis of Figure 2, there is an aspect that is important to discuss from the dynamic performance point of view: how could the modulation of P_{Wind} be performed to effectively decrease rotor angle excursions when a large disturbance occurs in the power system.

2.2. Time Response Analysis of a Grid-Side Voltage Source Converter (GSVSC) of a Wind Generator (WG) Unit during Large Disturbance Conditions

In current operational practice, when a large disturbance occurs in a power system with a high share of wind power levels, the WG units are expected to provide a certain level of transient voltage support. This is usually known as the low-voltage ride-through or fault ride-through (FRT) control function of the grid-side voltage source converter (GSVSC) of a WG unit [18]. As soon as a voltage dip in the power system is detected by the WG unit (i.e., by the GSVSC), the FRT control function is enabled, and it adjusts the current injected by the GSVSC into to the AC network. This adjustment usually priorities the reactive current over the active current generated by the GSVSC in order to transiently boost the voltage dip in the power system. The level of the reactive current injection provided by the GSVSC depends on the level of voltage deepness experienced by the power system.

For instance, some transmission system operators in Europe have already defined the level of reactive current injection during the period of a voltage dip in the transmission network [19] that it is expected from the FRT function of a the GSVSC unit. Thus, the PAM method (c.f. Section 3) can be seen as a complementary mechanism that works together to the FRT function during its activation and post-activation time periods.

Simply put, if during the fault period the FRT function allows a certain margin for the modulation of the active current of the grid-side VSC, a PAM controller can theoretically be conceived to take over of the active current modulation. Besides, when the FRT function is disabled (i.e., post-FRT period), the PAM controller will keep modulating the active current of the GSVSC for some additional seconds (e.g., 5–10 s as described in Section 3). Motivated by the observations from Figure 2, it is proposed that the PAM controller operates during the FRT and post-FRT periods. In this way, the power-angle curve can be affected (both in magnitude and phase), as a countermeasure against the performance shown in Figure 2b to move towards the performance shown in Figure 2a. In this way, the WG1 unit equipped with PAM controller can transiently support the rotor angle excursion exhibited by the nearby G1 unit.

The illustration of the expected performance of a PAM controller is presented through time-domain simulations executed considering the reduced power system shown in Figure 1. The dynamic model of the system was built in MATLAB Simulink R2019b® (9.7, MathWorks, Natick, MA, USA). In Figure 1, G1 is represented by a second-order model, whereas the WG1 type IV is represented by a controlled voltage source, to which the PAM controller (fundamentally modelled as a wash-out feedback loop, c.f. Section 3), is attached. The steady-state active power set-points of G1 and WG1 are defined as $P_{e_{SG}} = 0.5$ pu and $P_{Wind} = 0.5$ pu. The inertia (H) and damping constants of G1 are assumed to be 1 s and 0.005 pu, respectively. Additionally, it has been considered an adverse situation in which (cf. Figure 2b), $x_1 = 0.75$ pu, and $\frac{x_2}{x_1} = 0.75$. Figure 3 shows the results associated to the rotor angle response of G1 when a three-phase (bolted) fault at BUS 2, occurs at t = 1 s, and cleared after 200 ms with and without the PAM controller. The red (dotted) curve presented in Figure 3a reveals that the rotor angle stability of G1 is lost after the 200 ms fault at BUS 2 if, the PAM controller is not included (or enabled) in WG1. Conversely, if the PAM controller is activated in WG1, the response of the rotor angle of G1 presents a considerably faster damping response as shown by the green (continuous) curve Figure 3a. The explanation of this phenomena can be obtained by observing the active power responses presented in Figure 3b,c, respectively. Figure 3c, shows the two criteria used to execute the deployment of the P_{Wind} after the fault is released in the power system of Figure 1. The first criteria (suggested by [14,18]) recommends restoring the pre-fault active power levels as soon as possible after a three-phase fault occurs in the power system (i.e., WG1 without PAM). The second criteria is the one performed by the PAM controller in which, the transient management of the active power transfer in G1 (shown in Figure 3b) is induced by the modulation of P_{Wind} (shown in Figure 3c) affecting the θ_2 expressed in (2). In any case, it is revealed that the transient regulation of the active power of the WGs can transiently influence the amount of active power provided by the SGs (as shown in Figure 3), offering in that way a better solution to enhance transient stability response during and after a large disturbance rather than other power flow control devices (e.g., the phase-shifting transformers [20]).

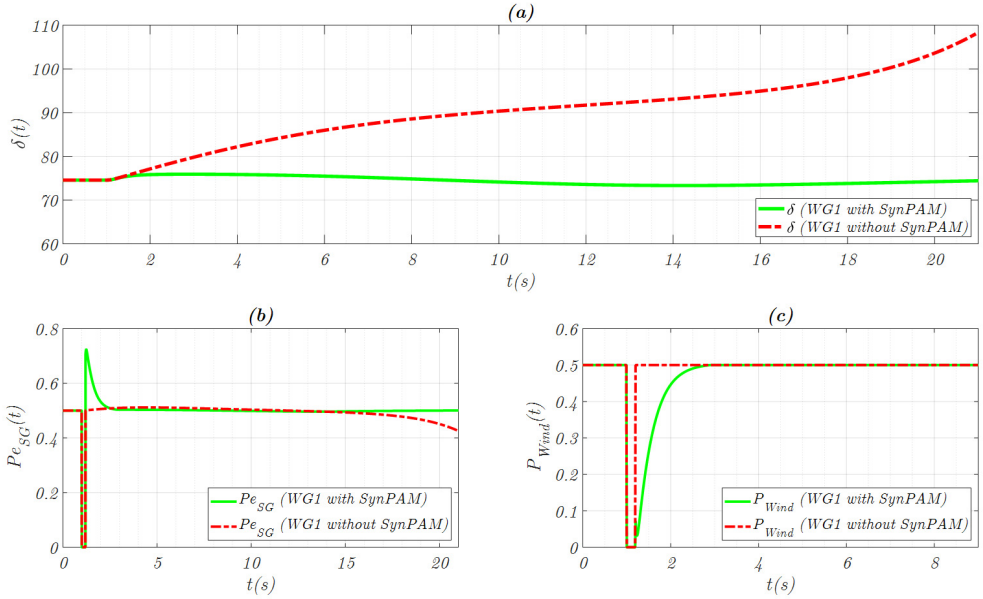

Figure 3. Rotor angle and the active power responses after a 200 ms three-phase fault (t = 1 s) at BUS 2 in Figure 1. (**a**) showing the time response comparison of δ having the PAM controller respectively enabled (continuous green line) and disabled (red dashed line) in WG1. (**b**) showing the active power transferred by the G1 unit by considering the PAM controller respectively enabled and disable in WG1. (**c**) showing the active power modulation response of the WG1 with and without PAM controller during and after the fault condition occurs.

3. The PAM Scheme in a High Share of Power Electronic Interfaced Wind Generation

In the power system industry, one of the solutions that has been widely accepted for executing a fast modulation of the SG's active power is known as the Power System Stabilizer (or PSS). This PSS solution proposes a way to directly modulate the SG's active power based on a control scheme that usually involves filter differentiators (or wash-out filters) and phase compensators (or lead-lag filters) [3]. The essence of this control scheme is to modify the SG's active power based on the measurement of the deviation of the rotational speed of the SG (connected to the power system) considering two aspects. The first one is to limit, the time delay effects associated to the inertia and the electromagnetic fluxes of the SG by means of the phase compensators, and the second one is to execute the modulation of the active power only outside of the steady-state's rotational speed (or nominal frequency) range by means of the wash-out filter [3]. However, considering that the power system landscape is currently evolving towards a set of generation units which are not based in the same physical principles (i.e., Faraday's law or electromagnetic induction law), the control schemes for modulating the active power in a power system need to be upgraded.

For instance, the active power modulation, in a power electronic converter station, can effectively contribute to mitigating (or damping) the power oscillations of a conventional SG unit. According to [21], this contribution is more pronounced if the active power in the converter station (i.e., GSVSC of WGs unit) is modulated in phase with the rotational speed of the SG and, if the WG unit is located electrically close to the SG which presents the (active power) oscillatory behavior. Although the study presented in [21] was based on a set of differential equations which defined the power system dynamic behavior, the influence of the algebraic variables of the power system were not considered. This consideration was a plausible one since the tools for estimating the state of these algebraic variables (in real time) were not sufficiently developed at that time. Thus, the PAM controller in a high share of power electronic interfacing wind generators is sketched through Figures 1 and 4.

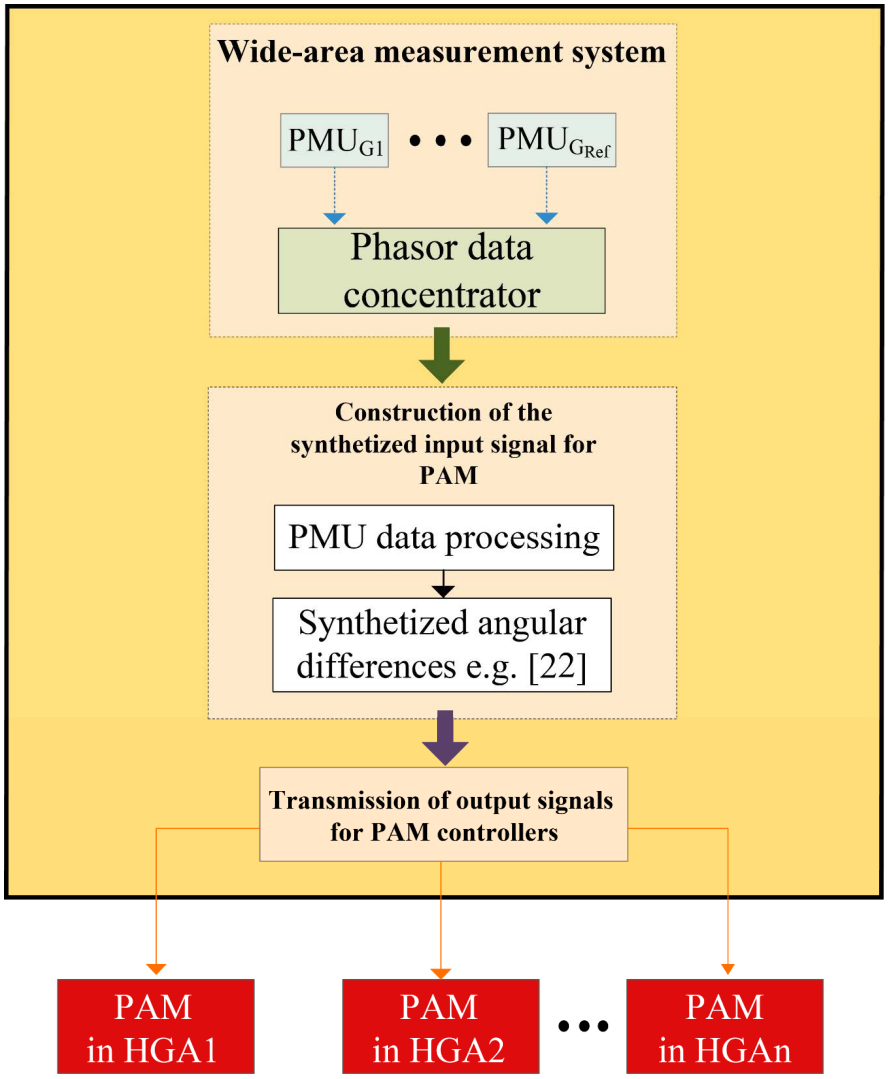

Figure 4. Flowchart of the real-time data provided by the PMUs for generating the rotor angle deviations required by each WG unit within their corresponding HGA.

3.1. Addition of the PAM Controller in a Type 4 WG

The implementation of the WG power plant model considered in this work has been based on the model of the IEC 61400-27-1 international standard for type 4 WG, as presented within the green box shown in Figure 5. The PAM controller modifies the active current provided by the WG plant when a large electrical disturbance (e.g., three-phase short circuit) occurs in a power system.

The purpose of the PAM controller is to alter the magnitude of the angular difference between the voltage at the terminal of the SG (i.e., G1 in Figure 1) and the voltage at the point of common coupling (i.e., BUS 2) of a nearby WG unit (WG1 in Figure 1). Therefore, by taking into account the small system shown in Figure 1 as an example, this can be interpreted as an attempt to alter the difference between δ and θ_2 (c.f. (2) and Figure 1) in order to generate a change in the active power transferred by the G1 unit to the power system (i.e., $P_{e_{SG}}$ in (2)). In principle, the PAM controller concept is implemented in the form of a reduced version of a PSS in which the phase compensation blocks have not been considered since the energy conversion process of the WG units do not rely on the electromagnetic induction law as discussed at the beginning of Section 3.

Moreover, the PAM controller can be attached either into the active power (P) regulation-loop of the WG (affecting the WG's active current reference) or in the reactive power (Q) regulation-loop

(affecting the WG's reactive current reference). Nevertheless, it was decided to attach the PAM controller just in the P-loop controller for two essential reasons.

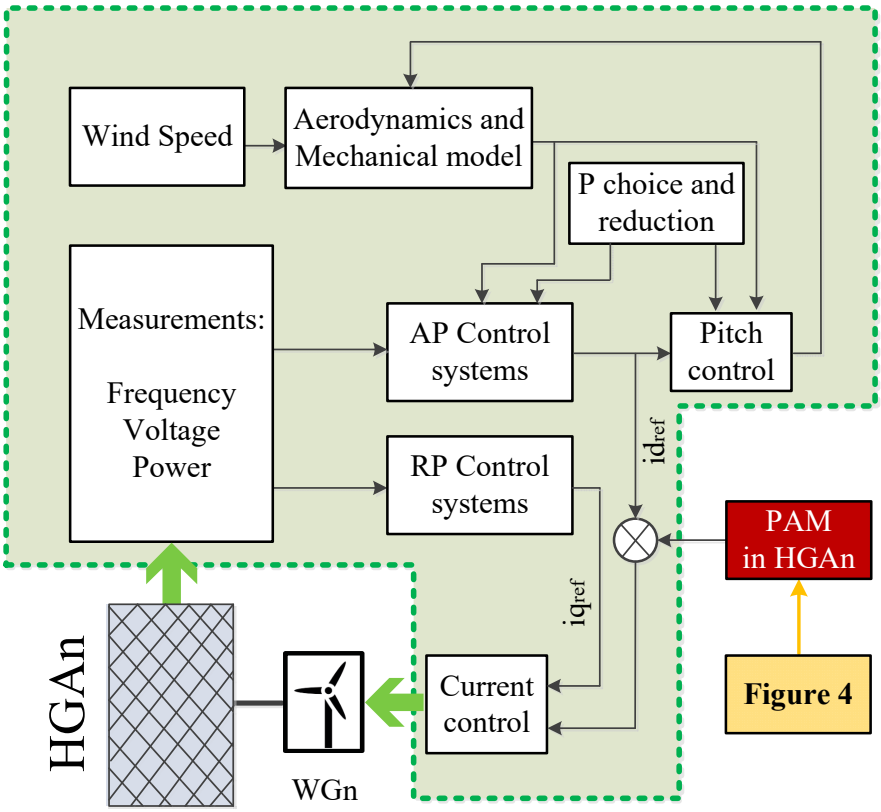

Figure 5. Control layout of the WG power plant located in the hybrid generation area n (HGAn) based on the The International Electrotechnical Commission (IEC) 61400-27-1 international standard (green box) in which the PAM controller has been included for modification of the WGn active (idref) current.

The first one is aligned with the fact that the phase angles and the active power sources are strongly linked as the sensitivity (Jacobian) matrix (of the power flow equations) indicates in a power system. This power–angle relationship can potentially be used by a WG unit to mitigate the effects of a large disturbance (e.g., three-phase fault), over the rotor angle response of a SG unit in a power system.

The second reason is based on the fact that the support obtained by the reactive power modulation of the WG unit would require large reactive power reserves for influencing the active power transferred by the SGs [23]. Such a case should be evaluated carefully, considering possible adverse implications with the (manufacturer specific) transient voltage support function (i.e., FRT function) implemented within the WG unit.

Figure 6, shows the structure of the PAM controller, which is superimposed on the output of the active power (P)-loop controller of a full converter type IV WG unit. As seen in Figure 6, the activation of the PAM controller starts right after the FRT function (i.e., Activation FRT flag in WG1) is activated. As mentioned before, the PAM controller in Figure 6 has the simple form of a filter differentiator (i.e., washout filter). Unlike typical PSS systems, the phase compensators (i.e., lead-lag filters) have not been included as part of the PAM controller structure, because a small phase lag between the active current reference and the active power output of the GSVSC is assumed.

The mitigation of the electromechanical oscillation of the SGs in a power system can be performed if the active power supplied by the converter station (i.e., GSVSC) is modulated in phase with the deviation of the rotational speed of the SG unit close to it [21]. This statement represents itself a design criterion for the PAM controller considering the ramp-rate's active power boundaries of the GSVSC, during a large disturbance in the power system.

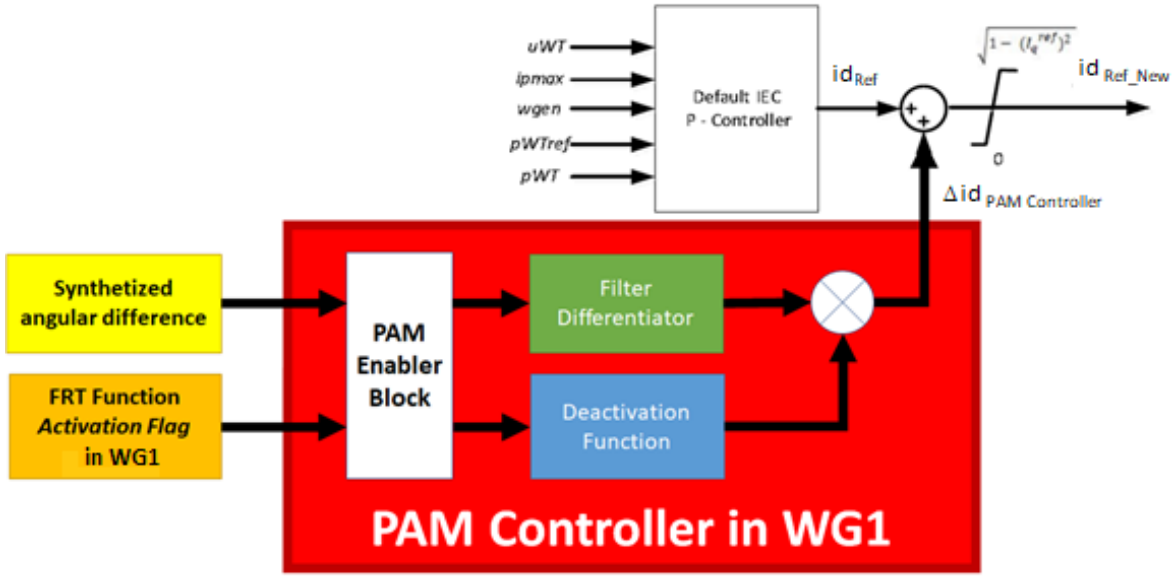

Figure 6. Basic structure of the PAM controller.

If the active power (i.e., active current reference of a WG unit) modulation needs to be in phase with the rotational speed of the SG electrically close, the most straightforward controller that can be used to perform this role is a proportional controller. On the other hand, the active power deployment of the WG unit should be executed in a smooth manner in order to avoid abrupt changes in the angular difference in the power system. This execution can be performed easily by including a first-order transfer function, as shown in (5) and (6) where $_{SG\_HGA\_i}$ represents the rotor angle deviation between the slack SG and the SG electrically close to the WG with the PAM controller and $P_{Wind\_HGA\_i}$ representing the active power deviation induced by the PAM controller. However, the first-order transfer function might create a phase shift difference between the active power and the rotational speed of the SG unit if its time constant (T) is chosen arbitrarily. For that reason, it is recommended that the values associated to this time constant (T) should be in the range of the ms period to minimize the phase difference and also to execute the deployment of the active power of the WG unit as soon as a large disturbance occurs in the power system.

$$\Delta P_{Wind\_HGA\_i} = \frac{Ks}{1+Ts}\Delta\delta_{SG\_HGA\_i} \tag{5}$$

$$\Delta\delta_{SG\_HGA\_i} = \frac{\Delta w_{SG\_HGA\_i}}{s} \tag{6}$$

Thus, from (5) and (6) it can be noticed that the performance of the PAM controller can be analyzed in two different ways depending on the input signal considered. The first way will define the active power changes (i.e., ΔP_{Wind_HGAi}) in the WG unit, based on a filter differentiator controller applied to the rotor angle deviation $\Delta\delta_{SG\_HGA\_i}$ as shown in (5). As shown in Figure 4, the synthetized rotor angle signal of the SG unit located in the HGA *i* (i.e., $\Delta\delta_{SG\_HGA\_i}$) is sent as an input signal for the PAM controller (c.f., (4)). This entails that the appropriate use of signal processing techniques (e.g., time delays and noise filtering) should be carefully considered for $\Delta\delta_{SG\_HGA\_i}$ since both factors will directly influence the performance of the PAM controller. Consequently, The signal-processing techniques considered in this work have been based in [22].

The second way of analyzing the performance of the PAM controller is based on the rotational speed response exhibited by the SG located in the HGA *i* when, a large disturbance occurs in the power system. If (6) is substituted in (5), the rotational speed deviation experienced by the SG_i unit (i.e., $\Delta w_{SG\_HGA\_i}$) will proportionally influence the active power supplied by the WG unit in the HGA

(i.e., $\Delta P_{Wind\_HGA\,i}$). This proportional power deviation and the rate of change of the active power of the WG unit are determined by the constants K and T in (5), respectively. However, it is relevant to mention that, as the goal of this study is focused on the enhancement of the transient (rotor angle) stability, the input signal considered in this work is the $\Delta\delta_{SG\_HGA\_i}$ signal. As an additional remark, the operation of the PAM controller is limited within a time period that is defined by a transfer function (deactivation function block in Figure 6) which progressively mitigates the influence of the PAM controller as soon as the post-FRT period in the WG unit begins. The time period can be adjusted by the constant T_{pFRT} (as shown in Figure 7), within the range in which the rotor angle excursions should be significantly attenuated, that is to say, within 15 s (according to [24]) after a large disturbance occurs in the power system.

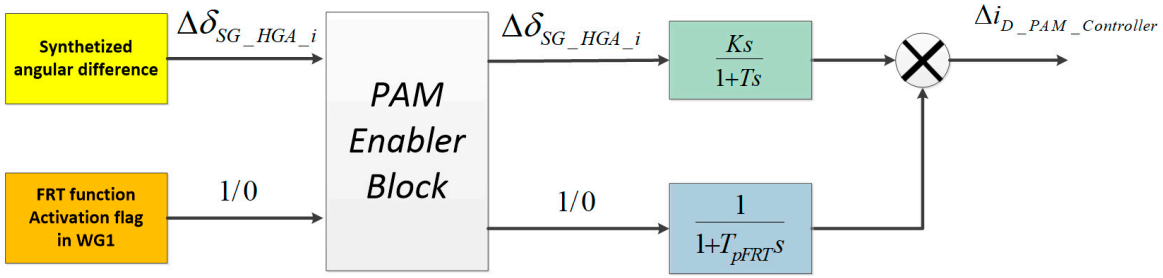

Figure 7. Internal control scheme of the PAM controller altering the active current modulation (during and after the fault period) based on the fault ride-through (FRT) function activation in the WG unit.

4. PAM Controller Assessment in Multi-Machine Power Systems Based on RMS Dynamic Simulations

This section shows several simulations experiments performed in the power system analysis software PowerFactory (2018, DIgSILENT, Gomaringen, Germany) in which the proposed PAM controller has been integrated within a modified version of the IEEE 9 BUS System, and a synthetic model of the Great Britain (GB) system. The goal is to show the effectiveness of the controller when the share of power electronic interfaced generation is increased above 50% of the total steady-state generation profile. The IEEE 9 BUS system is utilized as comprises only two synchronous machines. Therefore, the small size of the power system enables a good evaluation of the testing controller when different fault locations are performed. Additionally, for the synthetic model of the GB system, we will discuss and analyze if the implementation of the PAM controller should be necessarily included in each of the WG units within the multi-machine context like the synthetic model of the GB system.

4.1. Modified IEEE 9 BUS System

The modified IEEE 9 BUS System is shown in Figure 8. In the modified IEEE 9 BUS benchmark, WG1 is an aggregated model of 35 smaller wind generator units, while WG2 consists of 36 wind generator units. In this modified system, the inclusion of the PAM controller has been considered for just one of the two WG units presented in Figure 8, specifically in the WG1. The WG units provide 52% of the total active power generated by the energy as shown in Table 1. Additionally, it depicts the load flow results, with the loads being LA = 125 + j50 MVA, LB = 90 + j30 MVA, LC = 100 + j35 MVA.

Since in this case only two synchronous generators are present (i.e., SG1 and SG2), the selection of the input signal (i.e., rotor angle deviation) for the PAM controllers is relatively straightforward. As the synchronous generator SG1 represents the reference (slack) generator, the load angle of SG1 will constitute the angular reference for the PAM controller. Thus, the rotor angle deviation that will be fed into the PAM controller in WG1 is the rotor angle deviation of SG2 with respect to the rotor angle of SG1.

To illustrate the influence of the PAM controllers on the overall rotor angle stability of the system shown in Figure 8, three-phase faults with a fault clearing time (FCT) of 120 ms and a fault impedance

of 0.2 ohms, are applied at different buses of the system as shown in Figure 9. In Figure 9, the angular deviation produced by several three-phase faults events at buses 7, 8 and 9 are analyzed. Note from Figure 9e that the PAM control ensures (for all the fault events) fast damping of the rotor angle deviation between SG1 and SG2, if it is compared against the natural response of the system without having the PAM controller strategy enabled in WG1 as shown in Figure 9d.

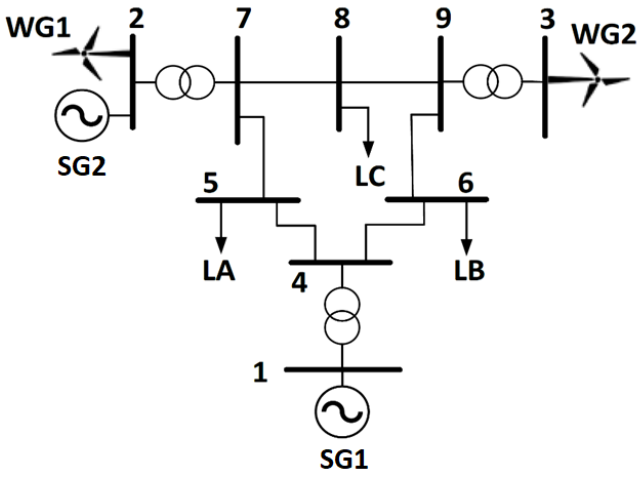

Figure 8. Modified IEEE 9 BUS System with 52% of wind power share.

Table 1. Load flow conditions of generator units in Figure 7.

Units	SG1	SG2	WG1	WG2
MW	73.02	81.5	81.5	85
MVAr	36.05	−4.6	0	0

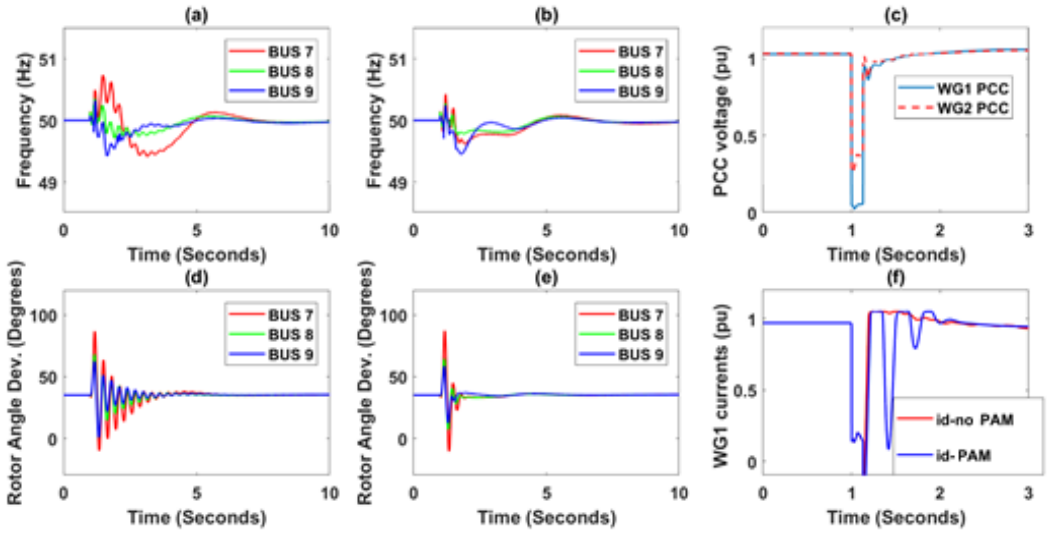

Figure 9. Faults implemented in the proximity of the wind turbines (**a**) frequency response without PAM controller enabled, (**b**) frequency response with PAM controller enabled, (**c**) voltage drop in the WGs point of common coupling (PCC) voltages for BUS 8 fault, (**d**) rotor angle deviations without PAM controller, (**e**) rotor angle deviations with PAM controller, (**f**) WG1 currents when BUS 7 is faulted.

Additionally, it is observed from Figure 9a,b that the PAM controller also helps in reducing the amplitude of the frequency deviation due to the variation of the active current (i.e., id current in Figure 9f), during and after the fault event occurs as described by the voltage drop in Figure 9c. Similar findings are observed when the study of the rotor angle deviation is extended, by considering

more fault cases in the system presented in Figure 8 (i.e., three-phase fault events at buses 4, 5 and 6) as shown in Figure 10.

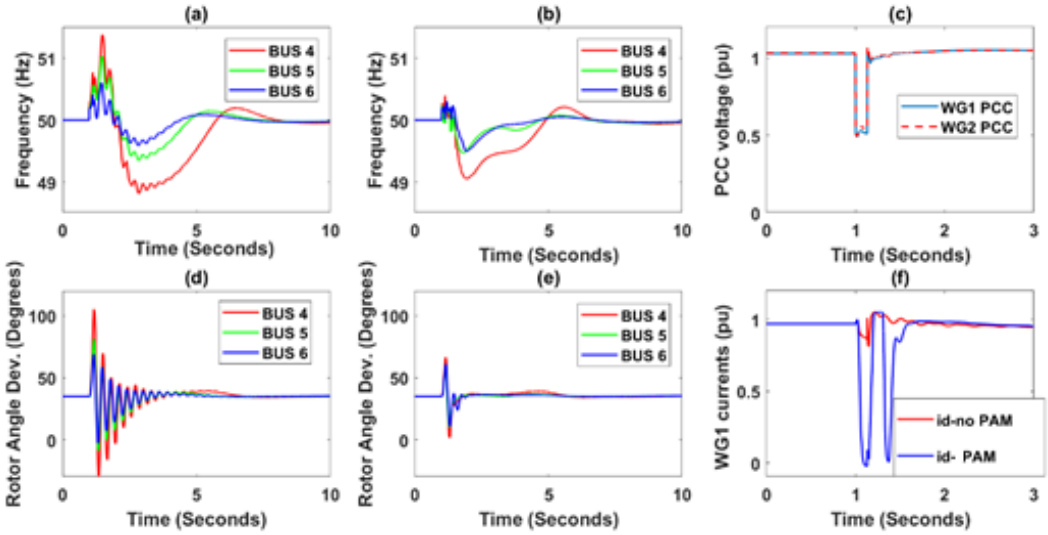

Figure 10. Faults implemented far from the wind turbines (**a**) frequency response without PAM connected, (**b**) frequency response with PAM connected, (**c**) voltage drop in the WGs PCC voltages for BUS 5 fault, (**d**) rotor angle deviations without PAM, (**e**) rotor angle deviations with PAM, (**f**) WG1 currents after BUS 5 fault.

If the results presented in Figures 9 and 10 are simultaneously analyzed, it can be seen that the location of the fault will influence the level of support provided to the rotor angle stability given by the PAM controller:

- Generally speaking, by comparing the shapes of the time responses presented in Figure 10d,e, it can be seen that the PAM controller quickly damps out the rotor angle oscillations and also, a reduction of the first angular swing. Likewise, if the Figure 9d,e are analyzed, it is again observed that a fast damping and a reduction of the first angular swing is produced in most of the fault cases.
- However, there can be some exceptions. For instance, when the fault at BUS 7 is particularly analyzed, it is found that the first angular swing presented in Figure 9e is very close to that observed in Figure 9d. This reflects that if the fault in the power system occurs very close to the WG having the PAM controller enabled, the level of support for the rotor angle stability provided by the WG will be diminished. This is aligned to the fact that the severe voltage dip that occurred at BUS 7 will induce the activation of the FRT function which will priorities the maximum reactive current injection during the fault period having no chances for modulating the active current of the WG during that period. Thus, the PAM controller can provide an effective rotor angle stability support (i.e., damping the rotor angle's oscillations) when the location of a three-phase fault is relatively far (i.e., a moderate voltage dip) from the WG having the PAM controller incorporated.

4.2. Comparison of the PAM Controller under a Real-Time Simulation Enviroment for Rotor Angle Stability Enhancement in a Small Multi-Machine System

As described in Sections 2 and 4.1, the PAM controller can theoretically enhance the response of the rotor angle oscillations experienced by synchronous generators when a large disturbance occurs in the power system. This enhancement is based on the increment of the damping characteristic (associated to the rotor angle oscillations of the SGs) driven by the active power modulation of the WG during and after a large disturbance is experienced by the power system. On the other hand, there are also other strategies that modulate the active power of a WG power plant under the same fault and post fault network conditions. Some of these other strategies are: the FRT function and the Voltage Dependent

Active Current (VDAC) reduction [25]. The aim of the FRT function has been already described in Section 2.2. However, the aim of the VDAC reduction is to provide certain frequency stability support (especially for low inertia networks) when a power unbalance (or fault condition) occurs in the power system. This support is carried out by modulating the active power provided by the WG power plant as a function of the voltage dip experienced at the PCC bus of the WG power plant [25].

Thus, the comparison of these two active power modulation strategies (i.e., FRT function and the VDAC) against the PAM controller is developed in this section as a way to illustrate the superior performance of the PAM controller in terms of the reduction of the damping time associated to the rotor angle responses when a power system is disturbed. Additionally, this comparison is carried out under a real-time digital simulation environment which is one of the simulation tools used nowadays by VSC manufacturers for the control algorithm's assessment of renewable energy systems to be connected to electrical power networks. More precisely, the modified IEEE 9 BUS benchmark system shown in Figure 8, has been implemented in the simulation platform NovaCor^{TM} (Version 5.003.3, RTDS Technology, Winnipeg, Canada) in which, the synchronous machines are represented as a 6th order generator model. Moreover, all the active power modulation strategies i.e., the FRT, the VDAC and the PAM controller, have been also implemented as described in [18,25] and Section 3.1, as part of the WG control layout presented in Figure 6. The load flow characteristics used in this simulation platform are identical to the ones mentioned in Table 1 and for the sake of simplicity, a 6 cycle three-phase fault at BUS 8 (c.f. Figure 8) has been considered.

The main simulation results for the analysis of the large disturbance event at BUS 8 under different active power modulation strategies are presented in Figures 11 and 12. The rotor angle response shown in Figure 12 reveals that the PAM controller, substantially enhances the damping characteristic of the angular oscillation of SG2 in Figure 8. This enhancement is indicated by the significant curtailment observed (around 7 s) in the settling time (i.e., faster damping time) associated to the rotor angle oscillatory behavior observed in the SG2 when the large disturbance occurs.

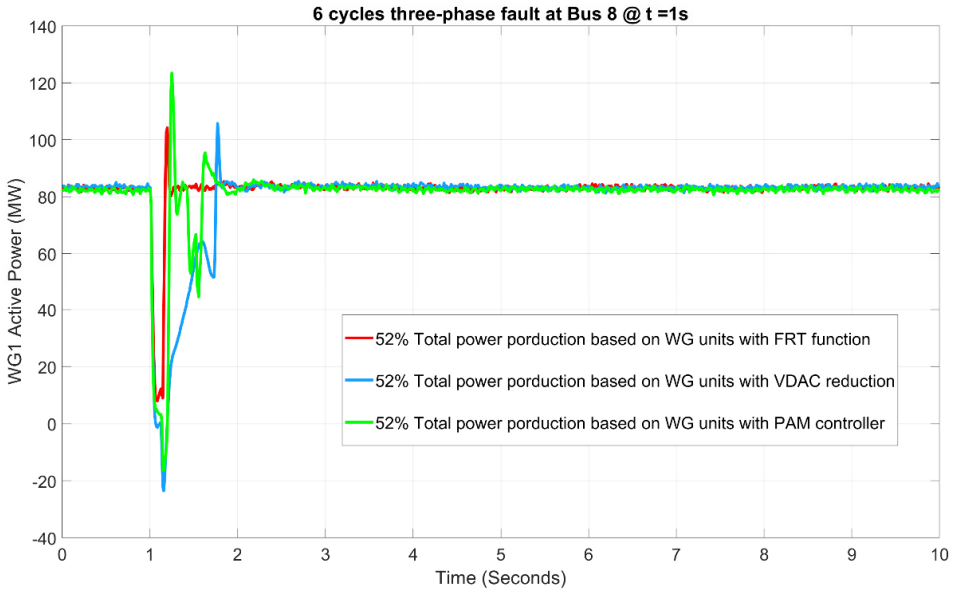

Figure 11. The active power deployments produced by the FRT function (red), the voltage-dependent active current (VDAC) reduction (blue) and the PAM controller (green) under a large disturbance event occurring at BUS 8.

It is also interesting to notice that even in a real-time simulation environment, for the transient (rotor angle) stability enhancement, the speed in which the post-fault active power is adjusted in the power system is as important as the active power shape during the post-fault period. This statement can be verified by observing the post-fault active power modulations presented in Figure 11.

The active power modulation conducted by the FRT function brings back the post-fault active power to its pre-fault level condition almost immediately, straight after the fault is released. However, this option produces the less-damped rotor angle response as shown in Figure 12. On the other hand, the VDAC reduction introduces a delay (based on a first-order transfer function) in the deployment of the post-fault active power as indicated in [25] to contribute to the frequency support of low inertia power systems. However, as indicated in Section 3.1, a frequency support strategy would not necessarily enhance the transient (rotor angle) stability feature of a power system has exhibit by the rotor angle response generated by the VDAC reduction in Figure 12.

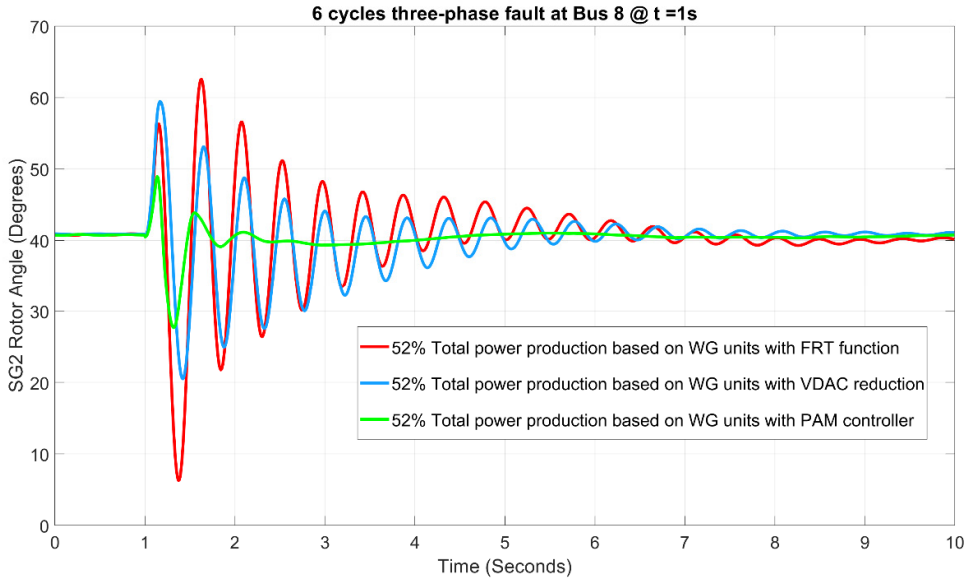

Figure 12. The rotor angle response of SG2 under the FRT function (red), the VDAC reduction (blue) and the PAM controller (green) when a large disturbance event occurred at BUS 8.

4.3. Description of the Synthetic Model of the Great Britain System

The synthetic model of the Great Britain (GB) system is examined to study the effectiveness of the PAM controller in a multi-machine system. In particular, the current study examines the Gone Green Scenario of 2030 for a 70% share of wind power generation described in [26]. The synthetic model of the GB system is shown in Figure 13 where, the way in which the generation units are located within the GB system is represented. This representation describes the generation units by using several colored zones. The black zones entail no generation units; the green zones represent only WG units, the blue zones constitute only SGs units and the red zones basically represent HGAs.

Following the same methodology used in the previous IEEE 9 BUS system, the PAM controller provides a rotor angle stability support for those SGs electrically close to the WG units (PAM controller-based) when a large disturbance occurs in a power system. This entails that the WG units located within the red zones previously described (c.f., Figure 13), are those in which the PAM controller is activated, that is to say, namely WG3, WG5, WG10, WG13, WG15, WG16, WG19, and WG20. Additionally, it is worth remembering (as explained in Section 3.1) that the PAM controller modulates the active power of the WG unit, depending on the angular difference between the SG (to be supported) and, the angular reference of the power system. Thus, the angular reference's location is a crucial factor to be considered when the information of the PMU devices, within the GB system, is processed. Nevertheless, the location of the angular reference can be a relatively easy task if the amounts of the inertia provided by each SG unit is individually compared, Thus when the inertia constant for each SG unit are compared, it is found that the SG unit with the highest inertia (8 s) in the GB system belongs to the SG11 unit. Therefore, the estimation (data) provided by the PMU in the red zone 11 (i.e., the rotor angle of the SG11 unit), represents the angular reference for all the

PAM controllers in the GB system. For the sake of illustration, it is worth mentioning that the inertia constant of the synchronous generators SG10, SG13, SG15, and SG16, is 7 s, whereas it is 2 s for synchronous generators SG3, SG5, SG7, SG8, SG19 and SG20. Moreover, the red zone 11 is the only one that exclusively comprises synchronous generation.

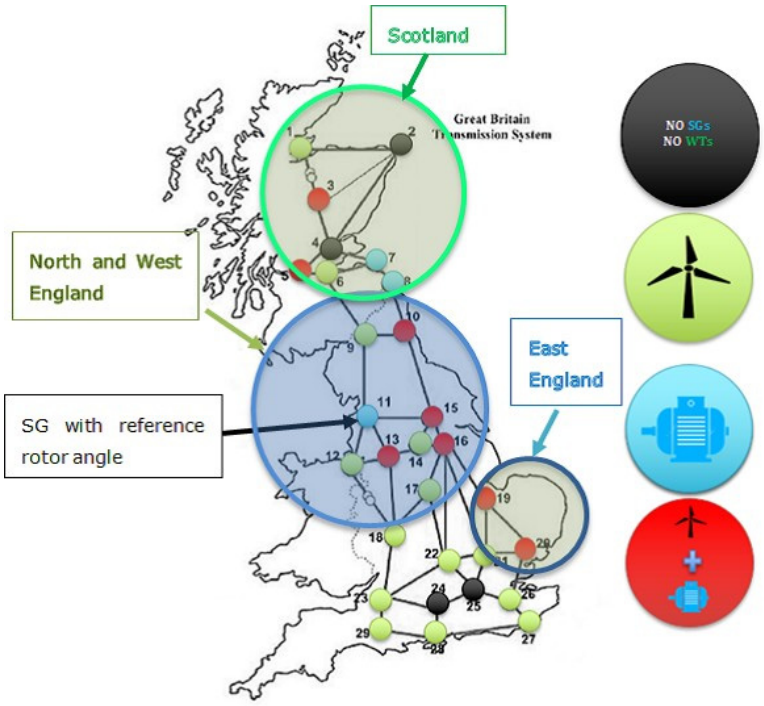

Figure 13. Geographical description of generation unit's location over the Great Britain (GB) power system.

The parameters of the PAM controllers (i.e., gains and time constants of washout filters), are determined based on a sensitivity analysis. In particular, all the controllers in a universal manner are iteratively changed based on an optimization function implemented as a software in Python (version 3.4, Python Software Fundation, DE, USA). The objective of the optimization function is the maximization of the key performance indicator (KPI) defined in [27] as shown in (7), where $\Delta\delta$ represents the angular difference of a SG with respect to the slack machine in the power system.

$$\mathrm{KPI} = 180 - \Delta\delta \tag{7}$$

After executing several time-domain simulations, the filter differentiator parameters for all the WG units having the PAM controller were obtained. It was found that a gain of K = 30 and a time constant of T = 0.01 s, incur maximum values of KPIs for both cases.

4.4. Fault Case for the Synthetic Model of the Great Britain System

In Section 4.1 the synthetic model of the GB system was described. In this section, the assessment of the PAM controllers within the WG units operating in a multi-machine context is presented. First of all, due to the characteristics of the network topology of the GB system and the inertia constants of the SG units, the fault event considered in this study is located in the Scottish region presented in Figure 13. As mentioned in the previous section, the inertia constants of the SG belonging to the Scottish region (i.e., SG3 and SG5), are comparatively low with respect to the other groups of SG units within the GB system.

Thus, if a 120 ms three-phase fault event is defined at the middle of the line 6–9, the resulting rotor angle deviations experienced by SG3 and SG5 will be quite pronounced as shown in the upper

left side of Figure 14. This pronounced rotor angle response is a consequence of the highest amount of apparent power transferred through that transmission line (i.e., line 6–9), during the pre-fault condition. Moreover, as shown in Figure 14, the fault at the line 6–9 is also influencing the rotor angle response of the SG units that do belong to the North, East and the West regions of the GB system (c.f., Figure 13). However, it can be noticed that even if the fault at line 6–9 does affect the rotor angle response of the SG units outside the Scottish region, the PAM controllers of the WG units (within all the red zones in Figure 13) also provide an appreciable damping effect for the rotor angle oscillations experienced by the rest of the SG units in the entire GB system.

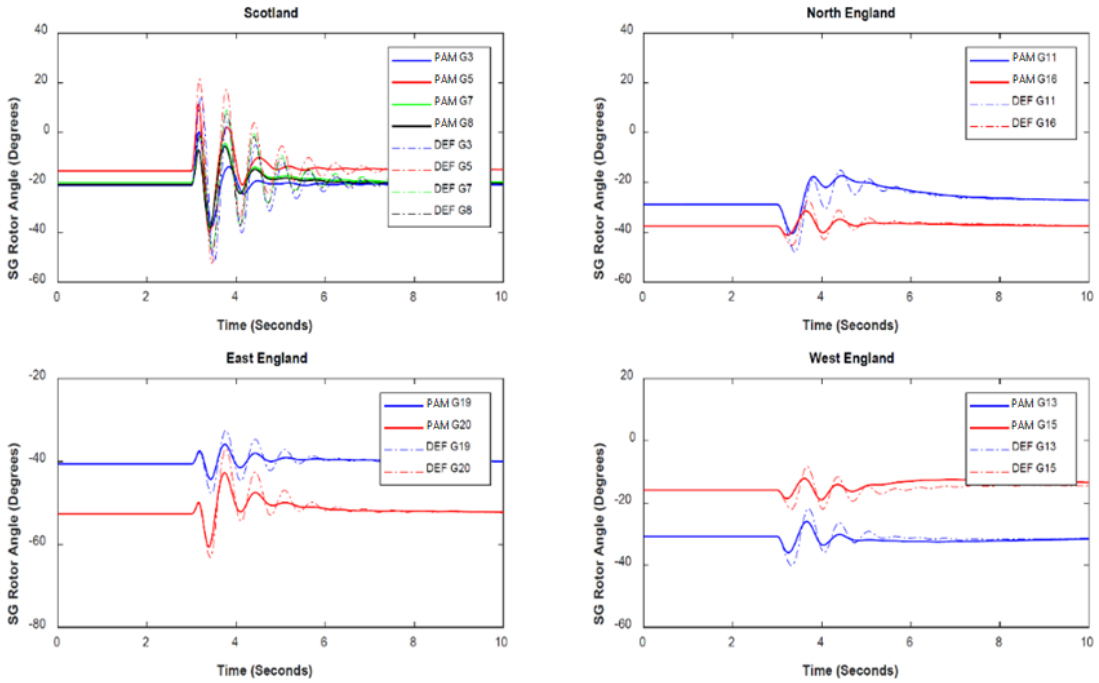

Figure 14. SGs' rotor angles responses for a 120 ms three-phase fault at Line 6–9 under a 66% share of wind generation in the GB system. Solid lines—WGs with PAM controller enabled, dashed lines—WGs without PAM controller enabled, default (DEF) response.

Up to now, all the WG units within the HGAs (indicated with red in Figure 13), are equipped with PAM controllers. However, as explained in Section 2.1 the PAM controller in general, it provides less support in terms of rotor angle stability when the HGA is electrically close to the angular reference of the system or the SG unit with the highest inertia (i.e., SG11). This statement can be verified for the multi-machine context of the GB system by developing simulation experiments (as shown in Figures 15 and 16) wherein all the HGA have the PAM controller enabled versus the case in which the PAM controller is only enabled in the farthest SG units with respect to the angular reference of the GB system (i.e., Scottish and Eastern England Areas in Figure 13).

Figures 15 and 16 show that the increase of damping is nearly the same when only the WGs units, within the low inertia areas (i.e., Scotland and East England), execute the PAM vs. the case in which all WGs within the HGAs execute the PAM. This entails that increasing the number of WGs with PAM should be done only if significantly higher FCT values are of interest an approach, however, bounded by the need of communication infrastructure for acquiring the measurements for every WG unit with PAM.

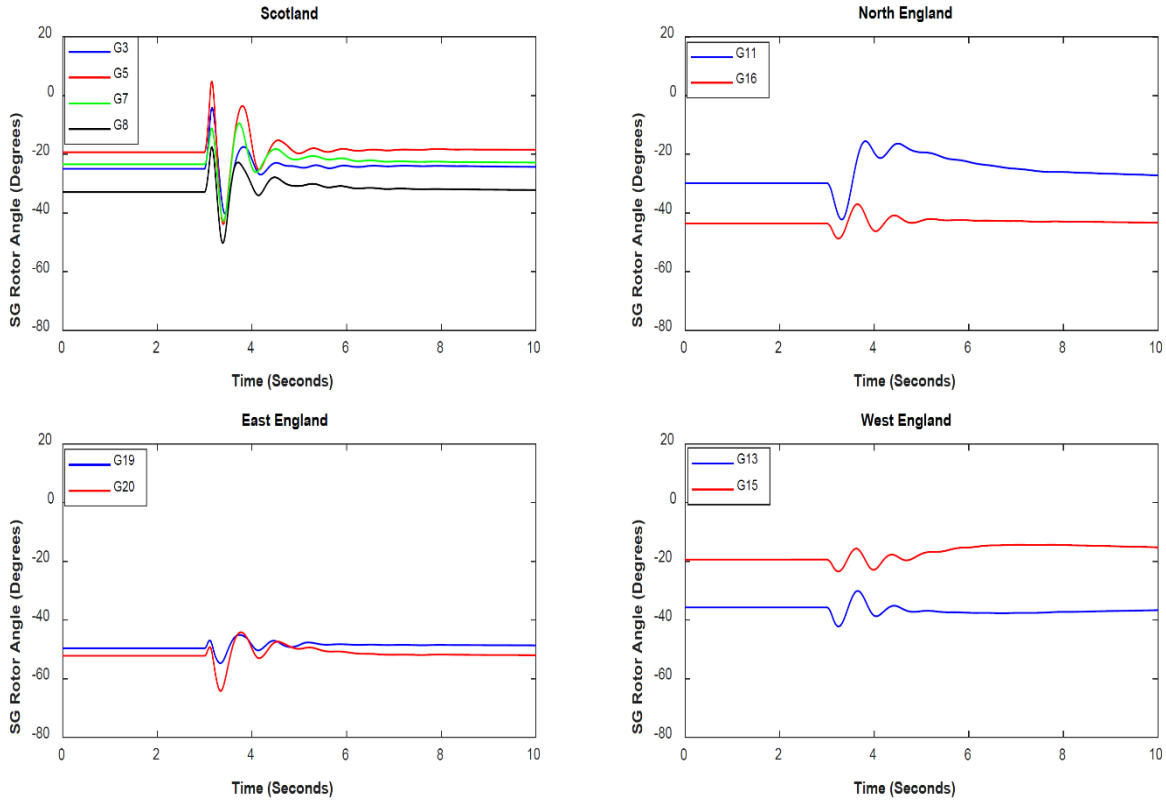

Figure 15. SGs' rotor angles' responses for a 120 ms three-phase fault at line 6–9 under a 66% share of wind generation in the GB system. Fault clearing time (FCT) = 120 ms. All WGs equipped with PAM controller.

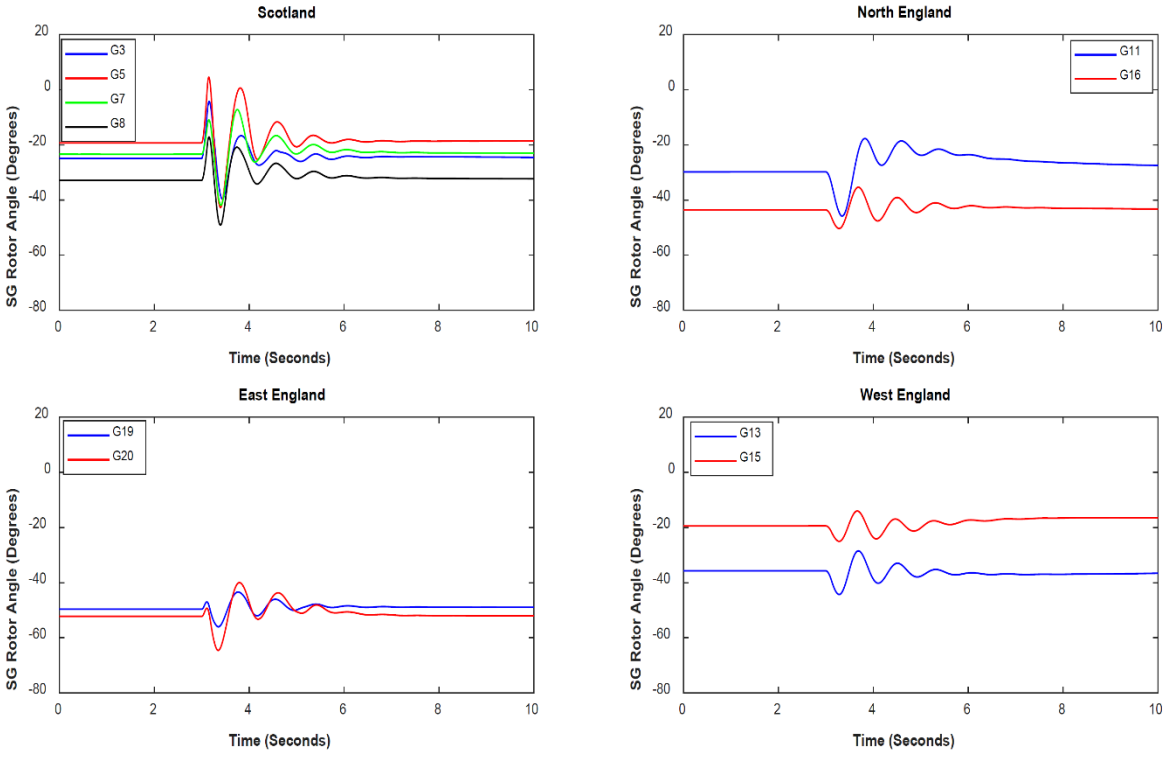

Figure 16. SGs' rotor angles responses for a 120 ms three-phase fault at line 6–9 under a 66% share of wind generation in the GB system. WGs with the PAM controller only activated in Scotland and the East England areas of Figure 13.

5. Conclusions

This paper presented an investigation of the design and effect of PAM controller addition on wind generators units, and their value for increasing the share of power electronic interfaced-generation without jeopardizing the large disturbance rotor angle stability performance of a power system. The main conclusions are summarized as follows:

The structure of the PAM controller proposed in this study evidences that wind generators (WG) can effectively contribute to mitigating large rotor angle excursions of synchronous generators by exploiting the available margin for active current modulation of the WG. The transient stability support was found to be higher (i.e., better mitigation of first swing magnitude and better oscillation damping) if the WGs with PAM controller are dominant in a synchronous area that is prone to transient instability issues. Furthermore, the transient stability is endangered in power systems with reduced inertia and lack of local resources for fast active power support (via fast modulation of active current injection), which is essential to mitigate the impact of a perturbation in the power balance (mechanical and electrical) of the synchronous generators.

For each PAM controller within each Hybrid Generation Area (HGA), the rotor angle difference between a nearby synchronous generator, and the reference machine (rotor angle reference) in the power system is used as the controller input signal. Simulation outcomes showed that these rotor angle deviations, as inputs of the PAM controller (attached to WG units), lead to an effective reduction of the magnitude of rotor angle's first-swing and a significant increase in the rotor angles' oscillation damping. These effects are more prominent when the faults occur in a distant location from the HGA that is prone to transient instability.

The application of a PAM controller in wind generators should also consider important aspects like: (i) the rotor angle is not directly available as measurement. Nevertheless, several methods for estimation of rotor angle from PMU data are already proposed [22]; (ii) not all WG units in a power system are required to be equipped with the PAM controller, i.e., WGs located electrically close to vulnerable SG units (prone to lose of synchronism) are of preferable for PAM.

Simulation results with the synthetic model of the GB system showed that significant improvement of transient stability performance could be achieved by using the PAM controller in conditions with a 66% share of wind generation. As a general observation, the addition of the PAM controller in renewable energy-based power plants should be considered when the traditional measures (including addition and/or re-tuning of PSSs) are not sufficient to ensure desired rotor angle response when a certain number of synchronous generators in conventional power plants has been decommissioned.

Author Contributions: Conceptualization, A.P.; Formal analysis, A.P.; Investigation, A.P.; Methodology, A.P. and S.P.; Resources, J.L.R.T.; Software, A.P.; Supervision, J.L.R.T., M.v.d.M. and F.G.-L.; Validation, J.L.R.T.; Visualization, E.R.; Writing–original draft, S.P.; Writing–review & editing, A.P. and J.L.R.T. All authors have read and agreed to the published version of the manuscript.

Funding: This research was carried out as part of the MIGRATE project. This project has received funding from the European Union's Horizon 2020 research and innovation program under grant agreement No 691800.

Acknowledgments: This research was carried out as part of the MIGRATE project. This project has received funding from the European Union's Horizon 2020 research and innovation program under grant agreement No 691800. This reflects only the authors' views, and the European Commission is not responsible for any use that may be made of the information it contains.

Conflicts of Interest: The authors declare no conflict of interest. The funders had no role in the design of the study; in the collection, analyses, or interpretation of data; in the writing of the manuscript, or in the decision to publish the results.

Abbreviations

The following abbreviations are used in this manuscript:

WG	Wind Generator
SG	Synchronous Generator
PAM	Power-Angle Modulation
PCC	Point of Common Coupling
GSVSC	Grid-Side Voltage Source Converter
FCT	Fault Clearing Time
PSS	Power System Stabilizer
MPPT	Maximum Power Point Tracking
LVRT	Low Voltage Ride Through
KPI	Key Performance Indicator
GB	Great Britain
IEEE	Institute of Electrical and Electronics Engineers
MVA	Mega Volt-Ampere
RMS	Root Mean Square

References

1. Seritan, G.; Porumb, R.; Cepisc, C.; Grigorescu, S.D. *Electricity Distribution-Intelligent Solutions for Electricity Transmission and Distribution Networks-chapter: Integration of Dispersed Power Generation*; Karampelas, K., Ekonomu, L., Eds.; Springer: Berlin/Heidelberg, Germany, 2016; pp. 27–61. ISBN 978-3-662-49434-9.
2. Porumb, R.; Seritan, G. *Green Energy Advances-chapter: Integration of Advanced Technologies for Efficient Operation of Smart Grids*; IET Inspec, EBSCO: London, UK; ISBN 978-1-78984-200-5. [CrossRef]
3. Kundur, P.; Paserba, J.; Ajjarapu, V.; Andersson, G.; Bose, A.; Canizares, C.; Hatziargyriou, N.; Hill, D.J.; Stankovic, A.; Taylor, C.; et al. Definition and Classification of Power System Stability IEEE/CIGRE Joint Task Force on Stability Terms and Definitions. *IEEE Trans. Power Syst.* **2004**, *19*, 1387–1401.
4. Huang, C.; Li, F.; Jin, Z. Maximum Power Point Tracking Strategy for Large-Scale Wind Generation Systems Considering Wind Turbine Dynamics. *IEEE Trans. Ind. Electron.* **2015**, *62*, 2530–2539. [CrossRef]
5. Cirrincione, M.; Pucci, M.; Vitale, G. Neural MPPT of Variable-Pitch Wind Generators with Induction Machines in a Wide Wind Speed Range. *IEEE Trans. Ind. Appl.* **2013**, *49*, 942–953. [CrossRef]
6. Shi, L.-B.; Sun, S.; Yao, L.; Ni, Y.; Bazargan, M. Effects of wind generation intermittency and volatility on power system transient stability. *IET Renew. Power Gener.* **2014**, *8*, 509–521. [CrossRef]
7. Lin, L.; Zhao, H.; Lan, T.; Wang, Q.; Zeng, J. Transient stability mechanism of DFIG wind farm and grid-connected power system. In Proceedings of the 2013 IEEE Grenoble Conference, Grenoble, France, 16–20 June 2013; pp. 1–9. [CrossRef]
8. Liu, S.; Li, G.; Zhou, M. Power system transient stability analysis with integration of DFIGs based on center of inertia. *CSEE J. Power Energy Syst.* **2016**, *2*, 20–29. [CrossRef]
9. Muyeen, S.M.; Takahashi, R.; Murata, T.; Tamura, J. Integration of an Energy Capacitor System with a Variable-Speed Wind Generator. *IEEE Trans. Energy Convers.* **2009**, *24*, 740–749. [CrossRef]
10. Wang, L.; Truong, D. Dynamic Stability Improvement of Four Wind Turbine Generators Fed to a Power System Using a STATCOM. *IEEE Trans. Power Deliv.* **2013**, *28*, 111–119. [CrossRef]
11. Geng, H.; Xu, D. Stability Analysis and Improvements for Variable-Speed Multipole Permanent Magnet Synchronous Generator-Based Wind Energy Conversion System. *IEEE Trans. Sustain. Energy* **2011**, *2*, 459–467. [CrossRef]
12. Aragüés-Peñalba, M.; Gomis-Bellmunt, O.; Martins, M. Coordinated Control for an Offshore Wind Power Plant to Provide Fault Ride Through Capability. *IEEE Trans. Sustain. Energy* **2014**, *5*, 1253–1261. [CrossRef]
13. Egea-Àlvarez, A.; Fekriasl, S.; Hassan, F.; Gomis-Bellmunt, O. Advanced Vector Control for Voltage Source Converters Connected to Weak Grids. *IEEE Trans. Power Syst.* **2015**, *30*, 3072–3081. [CrossRef]
14. Weise, B. Impact of K-factor and active current reduction during fault-ride-through of generating units connected via voltage-sourced converters on power system stability. *IET Renew. Power Gener.* **2015**, *9*, 25–36. [CrossRef]
15. Leon, A.E.; Alonso, G.E.; Revel, G.; Alonso, D.M. Wind power converters improving the power system stability. *IET Gener. Transm. Distrib.* **2016**, *10*, 1622–16333. [CrossRef]
16. Machowski, J. Power system dynamics and stability. *Fuel Energy Abstr.* **1996**, *37*, 195. [CrossRef]

17. CIGRE WG B4. Guide for the Development of Models for HVDC Converters in a HVDC Grid. Tech. Rep. 2014. Available online: https://e-cigre.org/publication/604-guide-for-the-development-of-models-for-hvdc-converters-in-a-hvdc-grid (accessed on 4 April 2020).
18. Van Der Meer, A.A.; Ndreko, M.; Gibescu, M.; Van Der Meijden, M.A.M.M. The Effect of FRT Behavior of VSC-HVDC-Connected Offshore Wind Power Plants on AC/DC System Dynamics. *IEEE Trans. Power Deliv.* **2015**, *31*, 878–887. [CrossRef]
19. Mohseni, M.; Islam, S. Review of international grid codes for wind power integration: Diversity, technology and a case for global standard. *Renew. Sustain. Energy Rev.* **2012**, *16*, 3876–3890. [CrossRef]
20. Van Hertem, D.; Rimez, J.; Belmans, R. Power Flow Controlling Devices as a Smart and Independent Grid Investment for Flexible Grid Operations: Belgian Case Study. *IEEE Trans. Smart Grid* **2013**, *4*, 1656–1664. [CrossRef]
21. Smed, T.; Andersson, G.T. Utilizing HVDC to damp power oscillations. *IEEE Trans. Power Deliv.* **1993**, *8*, 620–627. [CrossRef]
22. Echeverría, D.E.; Rueda, J.L.; Cepeda, J.; Colome, D.G.; Erlich, I. Comprehensive approach for prediction and assessment of power system transient stability in real-time. *IEEE PES ISGT Europe 2013* **2013**, 1–5. [CrossRef]
23. Martinez, C.; Joos, G.; Ooi, B.T. Power system stabilizers in variable speed wind farms. In Proceedings of the IEEE Power & Energy Society General Meeting, Calgary, AB, Canada, 26–30 July 2009; pp. 1–7.
24. Gibbard, M.J.; Pourbeik, P.; Vowels, D.J. *Small-signal Stability, Control and Dynamic Performance of Power Systems*; University of Adelaide Press: Adelaide, Australia, 2015.
25. Ndreko, M.; Rueda, J.L.; Popov, M.; Van Der Meijden, M.A. Optimal fault ride through compliance of offshore wind power plants with VSC-HVDC connection by meta-heuristic based tuning. *Electr. Power Syst. Res.* **2017**, *145*, 99–111. [CrossRef]
26. Deliverable D1.6. Demonstration of Mitigation Measures and Clarification of Unclear Grid Code Requirements, Technical Report of the Massive InteGRATion of Power Electronic Devices (MIGRATE) Project. Available online: https://www.h2020-migrate.eu/downloads.html (accessed on 4 April 2020).
27. Wang, D.; Torres, J.L.R.; Rakhshani, E.; Van Der Meijden, M. MVMO-Based Identification of Key Input Variables and Design of Decision Trees for Transient Stability Assessment in Power Systems With High Penetration Levels of Wind Power. *Front. Energy Res.* **2020**, *8*, 41. [CrossRef]